

Optimization of Saturation Pulse Length in Parallel Transmission based Amide Proton Transfer MRI for Oncology

Applications

Jochen Keupp¹, Osamu Togao², Jinyuan Zhou³, Yuriko Suzuki⁴, and Takashi Yoshiura²

¹Philips Research, Hamburg, Germany, ²Department of Clinical Radiology, Kyushu University, Fukuoka, Japan, ³Department of Radiology, Johns Hopkins University School of Medicine, Baltimore, MD, United States, ⁴Philips Electronics Japan, Tokyo, Japan

Introduction - Amide proton transfer (APT) [1] offers a novel route to sensitive MR molecular imaging of endogenous cytosolic proteins or peptides. The APT signal – quantified by the asymmetry of the magnetization transfer (MT) at +3.5ppm relative to water - reflects concentrations of amide (NH) containing proteins, which are significantly enhanced in active tumor tissue [2]. APT is expected to play an important role in delineation and classification of active tumor tissue for therapy planning and monitoring, e.g. for differentiation of radiation necrosis and active/recurrent tumor [3]. The length of RF saturation (T_{sat}) is a key for sensitivity, in particular at low protein concentrations. While the length of RF pulses is hardware-limited on clinical MRI systems (typically $T_{sat} < 1s$), a technique based on parallel RF transmission was demonstrated recently [4], which allows arbitrarily long RF pulses via amplifier alternation. With this novel degree of freedom for clinical protocol design, research on optimal RF saturation schemes is needed for particular APT applications. Chicken egg-white protein phantoms at different concentrations may be used for APT sequence optimization. However, a good phantom model is lagging for the complex situation in brain tissue, where MT effects of macromolecules and native MT asymmetry influence the optimal choice of APT parameters. In this work, the role of T_{sat} is studied in an APT phantom model. Furthermore, the effect of T_{sat} on APT contrast is assessed in an exemplary clinical brain tumor case.

Methods - The study was performed on a 3.0T clinical whole-body scanner (Achieva TX 3.0T, Philips Healthcare, NL) using an 8-channel head coil for signal reception and 2-channel parallel transmission via the body coil. The phantom consists of 7 vials (30 mL) filled with a mixture of pasteurized chicken egg-white (10% protein), water and Magnevist (Bayer Healthcare), with protein concentrations of 0.6% up to 7% which were adjusted to equal T_1 relaxation ($T_1 = 2.06 \pm 0.08$ s). Informed consent was obtained from the tumor patient (brain metastasis from esophageal cancer), and the protocol was approved by the institutional review board. Acquisition software was modified to alternate the operation of the two transmission channels during the RF saturation pulse [4], while each amplifier is active only within its specifications (pulse length $\leq 250ms$, duty-cycle 50%). RF shimming was applied for both, image homogeneity (excitation/refocusing pulses) and for saturation homogeneity via a B_1 calibration measurement. During the saturation pulse, the two transmission channels were operated with amplitudes adapted to obtain the same B_1 level (spatial mean) per channel. Saturation pulse-trains: 50ms sinc-gaussian elements, $B_{1,rms} = 2.0 \mu T$. 2D fast spin-echo sequences with driven equilibrium [5] refocusing were used: (i) phantom protocol: $T_{sat} = 0.8$ to 4s, $TR = 1$ to 4.2s, $TE = 4.8ms$, FOV (200mm)², matrix 168x162, voxel 1.2²x5 mm³, pixel bandwidth 410Hz, 10 off-resonance frequencies $S[\omega]$ around $\pm 3.5ppm$ (step 0.4ppm) and S_0 ($\omega = -160ppm$). (ii) brain protocol: $T_{sat} = 0.5/1.0/2.0s$, $TR/TE = 5s/6ms$, FOV (230 mm)², matrix 168², resolution 1.8x1.8x5 mm³, 25 x $S[\omega]$, $\omega = -6$ to 6ppm (step 0.5ppm) and S_0 , and 2 minutes scanning time. δB_0 maps for off-resonance correction were acquired separately (identical geometry, 2D GRE, $\Delta TE = 1ms$, $TR/TE = 15ms/8ms$, 16 averages, 33 sec), while carefully fixing the resonance frequency reference and shimming as well as using low gradient strength to minimize B_0 eddy current effects. Images at different frequency offsets were co-registered using rigid-body transformations to compensate for head motion. Maps of the MT asymmetry $MTR_{asym} = (S[-3.5ppm] - S[+3.5ppm])/S_0$ were calculated based on point-by-point interpolation for δB_0 correction [4].

Results and Discussion - Fig. 1 displays selected results (5 concentrations) of the phantom-based optimization of T_{sat} in terms of the relative gain to the contrast (MTR_{asym}) obtained at $T_{sat} = 0.8s$. At high protein concentrations (e.g. 7%), MTR_{asym} is increasing slowly with T_{sat} (due to the possible back-exchange), with a maximum gain of about 35-40% at $T_{sat} = 4.0s$. However, for low protein concentrations (1%), the signal gain is pronounced between $T_{sat} = 1s-2s$ (50-60%) and continues to rise slowly up to 70-80% at $T_{sat} = 4.0s$. This non-linear behavior will increase sensitivity to low amide concentrations at $T_{sat} \approx 2s$ and thus is expected to serve to detect and classify lower grade tumor tissue. However, increasing T_{sat} requires longer TR and reduces the contrast-to-noise (CNR) obtained in equal scan time. Doubling $TR(T_{sat})$ will decrease CNR by 40%, thus an overall CNR gain is expected between $T_{sat} = 1.5-2.0s$, depending on the target protein concentration range. It is important to perform T_{sat} optimization with equalized T_{1w} values, because $MTR_{asym} \propto (1 - \exp(-T_{sat}/T_{1w}))$ [1] (when back-exchange is negligible, as at low concentrations). Tumor tissue typically shows longer T_1 relaxation than normal brain tissue ($T_1 = 1.4$ to $1.8s$ at 3T), thus $T_{1w} = 2s$ was chosen here. Nevertheless, the phantom does not reflect the complex MT contrast behavior in brain tissue. The variation of T_{sat} in a clinical brain metastasis example (Fig.2 and Tab.1) shows a pronounced contrast increase from $T_{sat} = 0.5$ to 2s. MTR_{asym} is observed to increase with T_{sat} in the tumor by 55%, better reflecting the inhomogeneous tissue protein concentration. In addition, the signal from normal WM is decreasing and serves for a higher contrast. This single tumor case may only serve as a demonstration without statistical proof, but is very promising for further analysis in different tumor types. The results underline the importance to enable long T_{sat} on clinical scanners for sensitive APT-MRI and to optimize sequences under realistic conditions *in vivo*. Analysis in different tumor types can be pursued realistically using a set of 2D sequences, as shown here, while final clinical protocols will be performed in 3 dimensions.

References

1. Zhou J et al., Nat Med 9:1085 (2003)
2. Jones CK et al., MRM 56: 585 (2006)
3. Zhou J et al., Nat Med 17:130 (2011)
4. Keupp J et al., ISMRM 19:710 (2011)
5. Becker ED et al., J Am Chem Soc 91:7784(1969)

Figure 2: Increase of APT contrast with longer T_{sat} demonstrated on a human brain tumor (metastasis). (a) Metastasis and edema apparent in T2w image. (b) APT contrast in rainbow color scale for $T_{sat} = 0.5s$, (c) 1.0s and (d) 2.0s. Contrast is increasing by MTR_{asym} increase in the tumor and decrease in contralateral normal white matter.

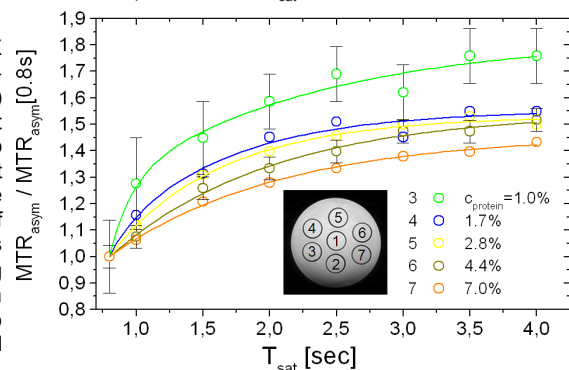


Figure 1: Optimization of RF saturation pulse lengths for APT using a protein concentration phantom with equalized T_1 relaxation. Particularly at low concentrations, about 50-60% signal gain is obtained by increasing T_{sat} from 0.8s to 2s. Because of the long required TR, scan time efficiency would decrease for long pulses above 2s.

Table 1:

APT contrast = $MTR_{asym} [\%]$ in a brain tumor for different RF saturation lengths.

MTR_{asym}	$T_{sat} = 0.5s$	$T_{sat} = 1.0s$	$T_{sat} = 2.0s$
Metastasis	3.6 \pm 0.5 % 2.3 ... 5.4%	4.6 \pm 0.7 % 2.2 ... 7.0%	5.3 \pm 1.2 % 2.3 ... 8.4%
Normal WM	1.6 \pm 0.6 %	0.9 \pm 0.6 %	0.6 \pm 0.6 %
Met - Normal	2%	3.7%	4.7%

